

Kinetic solvent isotope effects on the deacylation of specific acyl-papains

Proton inventory studies on the papain-catalysed hydrolyses of specific ester substrates: analysis of possible transition state structures

Ronald J. SZAWELSKI and Christopher W. WHARTON

Department of Biochemistry, University of Birmingham, P.O. Box 363, Birmingham B15 2TT, U.K.

(Received 9 June 1981/Accepted 10 August 1981)

1. The hydrolyses of the *p*-nitrophenyl esters of *N*-benzyloxycarbonylglycine, α -*N*-benzyloxycarbonyl-L-lysine and *N*-methoxycarbonyl-L-phenylalanyl-glycine catalysed by papain (EC 3.4.22.2) have been studied in solvents having a variable composition of $^2\text{H}_2\text{O}$ and H_2O . 2. k_{cat} , which represents deacylation in the papain-catalysed hydrolysis of reactive esters, is some 2.3-fold less in $^2\text{H}_2\text{O}$ compared with H_2O . The magnitude of k_{cat} has been determined as a function of the ^2H atom fraction of the solvent. 3. Both linear and non-linear methods of least-squares regression analysis have been applied to the data in order to obtain best-fit parameter values for several three-parameter models which express k_{cat} in terms of the ^2H atom fraction of the solvent. These models represent some possible modes of restructuring of the active site protonic configuration consequent upon transition state formation. 4. The results of curve fitting reveal an essentially linear dependence of k_{cat} upon the ^2H atom fraction, and it may therefore be concluded that the isotope effect originates from a single proton which is in the process of transfer in the transition state. 5. It is postulated on the basis of this and other evidence that the mobile proton is transferred from an attacking water molecule to the imidazole side chain of His-159 during tetrahedral intermediate formation. This has the effect of stabilizing the transition state and promoting catalysis. The role of His-159 in deacylation is therefore to provide general base catalysis. 6. Models that involve two or more protons, such as a two-proton relay system analogous to that proposed for the serine proteinases, or a multiproton 'medium' effect, are considered unlikely on the basis of the data reported in this paper. 7. A more detailed examination of possible transition state structures reveals that the only structure compatible with available experimental data and consistent with certain theoretical predictions is one in which the proton translocates in concert with reorganization of the heavy atom framework. In addition, the transition state vibrations of the mobile proton are strongly coupled to those of the heavy atoms. These properties of the transition state are also manifest in the transition state for the deacylation of serine proteinases.

Many approaches have been applied to the determination of the mechanism of papain (see e.g. Lowe, 1976; Angelides & Fink, 1978; Johnson *et al.*, 1981*a,b*). Solvent isotope studies have been restricted to measurement of the changes in rate

Abbreviations used: Z-Gly-Nph, *N*-benzyloxycarbonylglyciné *p*-nitrophenyl ester; Z-Lys-Nph, α -*N*-benzyloxycarbonyl-L-lysine *p*-nitrophenyl ester; Meo-Phe-Gly-Nph, *N*-methoxycarbonyl-L-phenylalanyl-glycine *p*-nitrophenyl ester; *n*, atom fraction of ^2H in the solvent; HAR, heavy atom reorganization; PT, proton transfer.

values that result upon complete replacement of exchangeable solvent protons with deuterons, i.e. the kinetic solvent ^2H isotope effect. The magnitude of the isotope effect on k_{cat} is approx. 2.2–3.3 for the papain-catalysed hydrolysis of substrates in which deacylation is rate-determining (e.g. esters) (Whitaker & Bender, 1965; Brubacher & Bender, 1966; Hinkle & Kirsch, 1970; Zannis & Kirsch, 1978). These authors have interpreted ^2H isotope effects of this magnitude as evidence for general base catalysis. However, although the existence of an isotope effect does imply that some protonic

restructuring occurs during the reaction, it does not provide information concerning either the number of protons involved or their environment. Such information is obtainable by making rate measurements not only in $^2\text{H}_2\text{O}$ and H_2O , but also in binary mixtures of the two solvents. From the dependence of the rate upon the atom fraction of ^2H in the solvent (n) it is possible, in principle, to resolve the number of protons and their individual contributions to the isotope effect, and thus construct a 'proton inventory' (Kresge, 1964; Gold, 1972; Schowen, 1977, 1978).

Schowen and his colleagues have introduced the proton inventory technique to the study of enzyme catalysis. They have carried out several proton inventory experiments on hydrolytic reactions catalysed by serine proteinases. Generally, single proton transfer has been found when simple substrates have been studied (Elrod *et al.*, 1975, 1980) but in cases where highly specific substrates were used dual concerted proton transfer was observed (Elrod *et al.*, 1975, 1980; Hunkapiller *et al.*, 1976). These proton transfers are assumed to occur amongst the Asp-His-Ser residues of the potential 'charge relay' systems of these enzymes. The above observations appear to apply to both acylation and deacylation. A similar situation has been shown to exist in the case of the amidohydrolases (Elrod *et al.*, 1975; Quinn *et al.*, 1980). X-ray crystallography reveals that the active site Asp-His-Ser triad in chymotrypsin (Blow *et al.*, 1969) is replaced in papain by Asn(175)-His(159)-Cys(25) (Drenth *et al.*, 1976). However, since the side chain of Asn-175 is presumably unable to accept a proton at physiological pH, this would not constitute a viable 'charge relay' system. However, several authors (Brocklehurst & Malthouse, 1978; Brocklehurst *et al.*, 1979a; Angelides & Fink, 1978) have pointed out that rotation about both the $\text{C}^\alpha\text{-C}^\beta$ and $\text{C}^\beta\text{-C}^\gamma$ bonds of the side chain of His-159 could take place consequent upon binding of specific substrates (or modifying reagents). This could bring the imidazole side chain into close proximity with the carboxyl group of Asp-158 to form a close analogue of the serine enzyme 'charge relay' system. Such rotation is implied by the observation of acid catalysis of amide substrate hydrolysis (Lowe & Yuthavong, 1971), cryoenzymological studies (Angelides & Fink, 1978), active site thiol group modification studies (Brocklehurst & Malthouse, 1978; Brocklehurst *et al.*, 1979a,b), and consideration of stereoelectronic constraints (Deslongschamps *et al.*, 1975). Evidence for the involvement of Asp-158 in the catalytic mechanism has come from recent work on pH-rate profiles (Allen *et al.*, 1978) and structure-reactivity correlations (Zannis & Kirsch, 1978). Consequently a charge relay system in papain is an intriguing possibility; it cannot be ruled out *a priori*.

Examples in enzyme catalysis of isotope effects that result from the involvement of many non-translating solvent protons each of which contributes only a small effect (as deduced by proton inventory analysis), have recently been reported (Venkatasuban & Silverman, 1980; O'Leary *et al.*, 1981). It is important that this 'medium' effect which may arise, for example, from a conformational change that produces a perturbation of many solvating water molecules, be considered as a possible cause of the observed isotope effect.

It is evident that any of the mechanisms described above may be responsible for the isotope effect observed for the deacylation of papain. Indeed it is possible to conceive of many further mechanisms, each of which differs in the nature of its protonic restructuring. Therefore, in order to make a distinction amongst the possible protonic mechanisms we have initiated a study of papain catalysis by utilizing the proton inventory technique. This paper describes such experiments on the papain-catalysed hydrolyses of the *p*-nitrophenyl esters of *N*-benzyloxycarbonylglycine, α -*N*-benzyloxycarbonyl-L-lysine and *N*-methoxycarbonyl-L-phenylalanyl-glycine. These substrates are specific and are subject to well-defined rate-limiting deacylation (Lowe, 1976). In addition to the delineation of the proton inventory, the results obtained have been interpreted in conjunction with other available evidence and certain theoretical considerations in an effort to characterize more precisely the structure of the transition state in terms of the degree of proton transfer and the extent of reorganization of the heavy atom framework; the relative contributions of these two factors to the reaction co-ordinate have been evaluated.

Materials and methods

Materials

Dithiothreitol, Z-Gly-Nph and acetonitrile were obtained from BDH. Acetonitrile was redistilled before use and dried over molecular sieve; $^2\text{H}_2\text{O}$ (99.8 atom% ^2H) was obtained from Aldrich and was used as such; Z-Lys-Nph was obtained from Sigma; and Meo-Phe-Gly-Nph ester was synthesized as follows.

L-Phenylalanine (10g), NaHCO_3 (10.2g) and methyl chloroformate (4.2ml) were stirred vigorously in a mixture of 100ml of ethyl acetate and 100ml of water for 3 h. The layers were separated, the aqueous layer being re-extracted with 50ml of ethyl acetate. The aqueous layer was adjusted to pH2 with conc. HCl and extracted with $2 \times 50\text{ml}$ of ethyl acetate. The solvent was removed by rotary evaporation and the resulting colourless oil was dried over P_2O_5 in a vacuum dessicator (yield 8g).

Meo-Phe (6g) was dissolved in 30ml of dry chloroform together with 3.7ml of triethylamine and the mixture was cooled to -5°C in an ice/NaCl bath. Ethyl chloroformate (2.6ml) in 20ml of dry chloroform was added dropwise over 15 min and the solution was stirred for a further 10min at this temperature. Glycine ethyl ester hydrochloride (3.7g) was added to the solution followed by triethylamine (3.7ml) in 20ml of dry chloroform which was added dropwise over 15 min. The solution was stirred for 2h, being allowed to come to room temperature after 30min and was subsequently extracted with $2 \times 50\text{ml}$ of water, $2 \times 50\text{ml}$ of 2% (w/v) NaHCO_3 , $2 \times 50\text{ml}$ of 0.1M-HCl and $2 \times 50\text{ml}$ of water. Chloroform was removed by rotary evaporation to yield a crystalline product (yield 6.3g).

Meo-Phe-Gly-OEt (5g) was dissolved in 30ml of acetonitrile/water (1:1, v/v) and cooled in ice. NaOH (8.1ml, 2M) was added dropwise over 20min and the mixture was stirred for a further 10min. Acetonitrile was removed by rotary evaporation and the resulting aqueous solution was extracted with $2 \times 25\text{ml}$ of ethyl acetate, acidified to pH 2 with HCl and again extracted with $2 \times 25\text{ml}$ of ethyl acetate. Rotary evaporation of the solvent yielded white crystals of the acid (yield 1.5g).

Meo-Phe-Gly (1g) was dissolved in 25ml of dry tetrahydrofuran and cooled to -4°C in an ice-NaCl bath. Dicyclohexylcarbodi-imide (0.73g) and *p*-nitrophenol (0.5g) were added and the mixture was stirred at -4°C for 30min and for a further 2h at room temperature after which acetic acid (0.1ml) was added. Dicyclohexylurea was removed by filtration and the solvent removed by rotary evaporation. The resulting yellow oil was dissolved in ethyl acetate, left to stand for 1h, filtered and extracted repeatedly with 2% (w/v) NaHCO_3 until the aqueous layer was almost colourless. The organic layer was dried over sodium sulphate, rotary evaporated and the resulting material was recrystallized from hexane/di-isopropyl ether. M.p. was 163°C and yield 0.62g. Calc. for $\text{C}_{19}\text{H}_{19}\text{N}_3\text{O}_7$: C, 56.85; H, 4.77; N, 10.47; found: C, 56.7; H, 4.9; N, 10.3%. The n.m.r. spectrum was consistent with the expected structure. The purity of the intermediates at each stage of the preparation was checked by t.l.c. (solvent: toluene/chloroform/methanol/acetic acid; (4:4:2:0.1, by vol.); in each case a single spot distinct from the starting material resulted.

Papain as a $2 \times$ crystallized suspension was obtained from Sigma. After activation at pH 6.0 for approx. 20–30min with 2mm-dithiothreitol and passage through Sephadex G-25 the enzyme was found to possess 0.4–0.6mol of thiol per mol of protein. Water was glass distilled and deionized, buffer salts and other reagents were obtained from the usual commercial sources.

Kinetic procedures and preparation of mixed isotopic solvents

Solutions of 0.2M-phosphate buffer having different values of the atom fraction of ^2H in the solvent (n) were prepared gravimetrically by mixing in appropriate quantities 0.2M-phosphate buffers made up in H_2O and $^2\text{H}_2\text{O}$. A constant buffer ratio was maintained in all mixtures. A quantity sufficient for 15–25 reactions was prepared for $n = 0$, and for 4–7 reactions for each of the other values of n ; altogether 13 different values of n between 0 and approx. 0.98 were used for each experiment. Exchangeable hydrogen atoms contributed by added buffer salts were taken into account in the calculation of n . The pH and $p^2\text{H}$ values of the stock solutions of H_2O and $^2\text{H}_2\text{O}$ buffers (i.e. $n = 0$ and 0.98) were checked on a Radiometer pH meter model no. 26 and the $p^2\text{H}$ value was calculated using the relation $p^2\text{H} = \text{meter reading} + 0.4$ (Glascoe & Long, 1960). Papain (0.014–0.021mM) was activated in 0.05M-phosphate buffer, pH 6.0, containing 1mM-EDTA and 2mM-dithiothreitol for approx. 20–30min at room temperature and stored on ice; the resulting stock solution was stable for the duration of each experiment (approx. 6–8h). Substrate stock solutions were made up in dry acetonitrile [except for the stock solution of Z-Lys-Nph, in which 5% (v/v) water was included in order to enhance solubility] and stored on ice.

A typical kinetic run was performed as follows: a cuvette containing 2ml of buffer was brought to thermal equilibrium in the sample compartment of a Pye Unicam SP.1800 u.v. spectrophotometer thermostat-controlled at $25 \pm 0.1^{\circ}\text{C}$; $50\mu\text{l}$ of enzyme stock solution was then added. After thermal equilibration had been achieved, as judged by the response of a thermistor probe inserted directly into the cell, reaction was initiated by addition of $50\mu\text{l}$ of substrate, and the progress of the reaction was monitored at 400nm (340nm for Z-Lys-Nph). The pL change [the term pL refers to the apparent pH of an $\text{H}_2\text{O}/^2\text{H}_2\text{O}$ mixture, after applying the glass electrode correction (Glascoe & Long, 1960)] attendant upon reaction was checked in several cases and found to be negligible. For each n value, the aqueous rate of hydrolysis of the particular substrate was determined by substitution of $50\mu\text{l}$ of 0.05M-phosphate buffer, pH 6.0, containing 1mM-EDTA and 2mM-dithiothreitol, for enzyme stock solution. The rate values thus obtained, which varied slightly with n and in no case exceeded 5% of the total rate in the presence of enzyme, were fitted to a linear function of n by least-squares regression. Rate values measured in the presence of enzyme were corrected for aqueous hydrolysis by subtraction of the calculated aqueous rate. The reaction was followed to completion in several cases, and the total

change in absorbance (and hence $\Delta\epsilon$) was determined at several n values. $\Delta\epsilon$, which was found to decrease upon complete isotopic substitution of solvent by approx. 4% at pH 7.0 and approx. 6% at pH 6.0, was also fitted to a linear function of n , and a further correction was made.

Since the buffer ratio is constant in each mixed isotopic solvent, and the pK_a change of phosphate upon deuteration of solvent (Schowen, 1978) is approximately equal to the corresponding pK_a change of deacylation (Brubacher & Bender, 1966), $k_{cat.}$ will be situated at the same relative point on the $k_{cat.}$ -pL profile for each value of n . In view of the fact that the pH values at which rate measurements were made fall upon the plateau region of the $k_{cat.}$ -pH profile for deacylation, the sensitivity of $k_{cat.}$ to change in pL will be small in any case.

The kinetic parameters for the papain-catalysed hydrolysis of Meo-Phe-Gly-Nph at pH 7.0 and 25°C were determined by the method of Atkins & Nimmo (1973). The K_m and $k_{cat.}$ values were found to be 0.97 μM and 7.9 s⁻¹ respectively. The K_m values at pH 6-7 for Z-Gly-Nph and Z-Lys-Nph are 9.3 μM (Kirsch & Ingelstrom, 1966) and 1.71 μM (Bender & Brubacher, 1966) respectively, and consequently the initial substrate concentrations used in the experiments reported in this paper (Table 1) are much greater than the corresponding K_m values, and the initial phase of the reaction obeyed zero-order kinetics for all three substrates, with initial rate = $V_{max.} = k_{cat.}[E]_0$.

Theory and statistical analysis of data

Theory. The deacylation of papain in mixtures of ²H₂O and H₂O may be represented by Scheme 1. In this scheme it is assumed that a single proton, which is freely exchangeable with solvent, participates in the catalytic mechanism. This represents a particular case of the general situation in which several exchangeable protons participate in the reaction. The single proton case is used initially in order to introduce the fundamental concepts involved and will subsequently be extended to the general case.

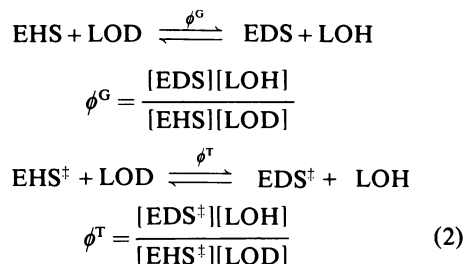
In this scheme EHS represents the fully protiated acyl-enzyme (ground state), EHS[‡] represents the fully protiated transition state for deacylation, EH represents the fully protiated free enzyme, P rep-

resents the carboxylic acid product formed by hydrolysis of the acyl-enzyme, K_H^\ddagger is the pseudo-equilibrium constant for transition-state formation, $k_B T/h$ (where k_B = Boltzmann's constant, T = temperature and h = Planck's constant) equals the rate constant for decomposition of the transition state into products, in accordance with the theory of absolute reaction rates (Eyring, 1935), and the species containing D represent the equivalent deuterated species.

It can be shown (Kresge, 1964; Gold, 1972; Alberty, 1975) that in this case the deacylation rate constant, k_n , is related to the ²H atom fraction (n), by eqn. (1):

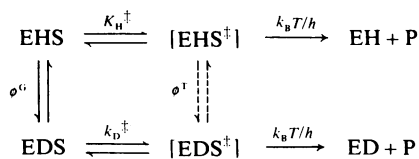
$$k_n = k_0 \frac{(1 - n + n\phi^T)}{(1 - n + n\phi^G)} \quad (1)$$

where k_n = rate constant for arbitrary atom fraction n , k_0 = rate constant for atom fraction 0, and ϕ^G and ϕ^T are equilibrium constants for the deuteration of the hydrogenic site in the ground state and transition state respectively, and are defined by eqns. (2).



where L represents either H or ²H. Accordingly, the ϕ values defined above represent the extent to which ²H fractionates between a particular hydrogenic site and a corresponding site on a solvent molecule, and for this reason are known as fractionation factors. In particular, the fractionation factor is equal to the ratio of ²H to H present on the particular site in a 1:1 mixture of H₂O and ²H₂O. Ground state fractionation factors, which are directly measurable for simple organic molecules (although this is extremely difficult for enzymes), have values characteristic of the chemical nature of the hydrogenic site, and are usually similar for the same functional groups in different molecules.

Transition-state fractionation factors are not directly measurable, and since the transition state has a very short lifetime it is not capable of direct proton exchange with the solvent. However, the transition state will be in pseudo-equilibrium with the solvent via the ground state equilibrium (see Scheme 1). If the proton is not in the process of transfer in the transition state but its microenvironment is altered during the reaction, its fractionation factor will have a value in between that of the ground state and that of the product, depending on the position of



Scheme 1

the transition state on the reaction co-ordinate. The resulting isotope effect is described as secondary in contrast to the primary effect which arises from a proton which is in the process of transfer in the transition state. If the proton is undergoing transfer, then its transition state fractionation factor is expected to be in the range 0.1–0.7 (see the Discussion).

As mentioned above, if several protons participate in the reaction, it is necessary to introduce additional equilibria into Scheme 1. In this case, eqn. (1) becomes eqn. (3), which is known as the Gross–Butler equation (Kresge, 1964; Gold, 1972):

$$k_n = k_0 \frac{\prod (1 - n + n\phi_i^T)}{\prod (1 - n + n\phi_i^G)} \quad (3)$$

where ϕ_i^G is the ground state fractionation factor of the i th exchangeable hydrogenic site, ϕ_i^T is the corresponding transition state fractionation factor, and ν is the number of protons involved in the reaction. Clearly protons unchanged during the reaction may be included in eqn. (3) but the terms in the numerator and denominator contributed by each of these protons will cancel. A detailed discussion of the validity of the assumptions implicit in the derivation of eqn. (3) is given by Gold (1972).

Consideration of eqn. (3) reveals that variation of n should, at least in principle, allow the determination of the value of ν and the ϕ_i^G and ϕ_i^T values. In practice, the presence of protons producing small effects may be obscured by experimental error. The construction of a 'proton inventory', which is what analysis of eqn. (3) as above implies, should allow a detailed description of the proton dynamics of the reaction. Clearly measurements restricted to $n = 0$ and 1 will not allow such a detailed analysis to be achieved.

Statistical analysis of data. In order to determine the proton inventory for a given reaction it is necessary to consider a number of specific forms of eqn. (3) (models) which encompass a variety of conceivable protonic mechanisms. If a number of models which covers a sufficient range of mechanisms is selected, it should be possible to specify the parameters of eqn. (3) for the reaction. This approach has been adopted in this paper, and three models have been fitted by least-squares methods to each of the sets of data obtained in the present studies.

The first model (Model I) describes a mechanism that involves two protons whose ground state fractionation factors are both set to unity. Eqn. (3) then becomes eqn. (4):

$$k_n = k_0(1 - n + n\phi_1^T)(1 - n + n\phi_2^T) \quad (4)$$

which may be rewritten as eqn. (5):

$$k_n = k_0 + k_0[(\phi_1^T - 1) + (\phi_2^T - 1)]n + k_0(\phi_1^T - 1)(\phi_2^T - 1)n^2 \quad (5)$$

Thus, linear least-squares regression analysis (Draper & Smith, 1966; Cornish-Bowden, 1976) may be employed to determine the values of \hat{k}_0 , $\hat{\phi}_1^T$ and $\hat{\phi}_2^T$, which are the best-fit estimates of k_0 , ϕ_1^T and ϕ_2^T respectively, and their variances and co-variances. Furthermore, it is possible to calculate the boundaries circumscribing joint confidence regions for the two parameters, ϕ_1^T , ϕ_2^T , at any given level of significance, by use of eqn. (6) (Box & Hunter, 1962; Draper & Smith, 1966):

$$SS(K_0, \phi_1^T, \phi_2^T) = SS(\hat{k}_0, \hat{\phi}_1^T, \hat{\phi}_2^T) \left[1 + \frac{p}{(m-p)} F(p, m-p, 1-\alpha) \right] \quad (6)$$

where SS is the sum of squares of residuals, m is the no. of data points, p is the no. of parameters, and $F(p, m-p, 1-\alpha)$ is the corresponding upper 100 $\alpha\%$ point of the F-distribution.

If k_0 is very accurately defined (see later), it may be treated as a constant, and eqn. (6) may be rearranged to give a quadratic equation in ϕ_1 and ϕ_2 that contains summations which have already been evaluated in the course of linear regression. Thus, for a given value of ϕ_1^T , eqn. (6) may be solved to produce two values of ϕ_2^T , with only a small amount of additional computation. It is therefore possible to generate a set of ϕ_1 , ϕ_2 pairs satisfying eqn. (6) and forming, in $\phi_1^T - \phi_2^T$ space, a locus encompassing all solutions, each defined by a point, which are consistent with the data at the given level of significance. This process may then be repeated for several different levels of significance, to produce a series of 'constant-confidence contours', as shown in Fig. 2.

The second model (Model II) to be tested describes the case of a single proton whose ground state fractionation factor is allowed to vary. Such a situation is described by eqn. (7):

$$k_n = k_0(1 - n + n\phi_T)/(1 - n + n\phi_G) \quad (7)$$

Best-fit values of k_0 , ϕ_G and ϕ_T , and their variance and co-variances were obtained by non-linear least-squares regression analysis which was performed using a combination of the simplex method of Nelder & Mead and the method of steepest descent (Wharton *et al.*, 1974).

The third model (Model III) to be tested is described by eqn. (8):

$$k_n = k_0(1 - n + n\phi)^\omega \quad (8)$$

This equation represents mechanisms that involve several protons with identical transition state fractionation factors with associated ground state fractionation factors of unity, or *vice versa*. In the former case, ω will be a positive integer, while in the latter case it will be a negative integer. If the fractionation factors are not equal, the best-fit value of ω will be non-integral. In this case eqn. (8) cannot correctly represent the true mechanistic situation, but may nonetheless be of diagnostic utility in discriminating amongst alternative mechanisms.

The choice of models outlined above was found to be adequate for the purpose of distinguishing the possible alternative mechanisms for the deacylation reactions described below. It is to be emphasized, however, that more complicated models would have to be applied to more complex cases, e.g. mechanisms involving many protons with different fractionation factors in the ground and transition states, in which case forms of eqn. (3) containing four or more parameters would have to be used (e.g. see Hopper *et al.*, 1973).

Results

In Table 1 are shown the best-fit values of k_0 , ϕ_1^T and ϕ_2^T for model I. The data for Z-Lys-Nph are shown as an example in Fig. 1, together with the best-fit curve for model I. For all three substrates it is apparent that ϕ_1^T is close to unity while ϕ_2^T ranges between 0.40 and 0.44. The best-fit value of k_0 is very well defined (s.e.m. 0.5–0.7%) and it is therefore possible to display the results for model I in the form of a two-dimensional contour diagram in parameter space (see the section on statistical analysis of data). As an example, the results for Meo-Phe-Gly-Nph are shown in Fig. 2. Since model I is symmetric in ϕ_1 and ϕ_2 , the contour map will possess a line of symmetry, namely $\phi_2 = \phi_1$, and a second solution, exactly equivalent to the first, will exist as the reflection of the first in the line $\phi_2 = \phi_1$.

The best-fit parameters for model II (Table 2) show that for all three substrates the ground state fractionation factor is close to unity whereas the transition state fractionation factor is again 0.40–0.44.

Finally, fitting of model III (Table 3) yields values of 0.35–0.44 for ϕ and a value of ω close to +1.0.

It is clearly apparent from Tables 1–3 and Figs. 1 and 2 that the curve-fitting has resulted in the resolution of all three models I–III to a linear or near-linear form, i.e.:

$$k_n = k_0(1 - n + n\phi^T)$$

The significance of small deviations from unity seen in the ϕ_1^T values in Table 1, ϕ_G values in Table 2 and ω values in Table 3 cannot be rigorously assessed owing to the possible introduction of small errors as a result of the procedures used to correct the rate values for the variation of $\Delta\epsilon$ and the aqueous rate with n . Such errors could arise since the variation of the aqueous rate and $\Delta\epsilon$ with n is small, and it was not possible in either case to make a distinction between a linear and slightly curved dependence upon n .

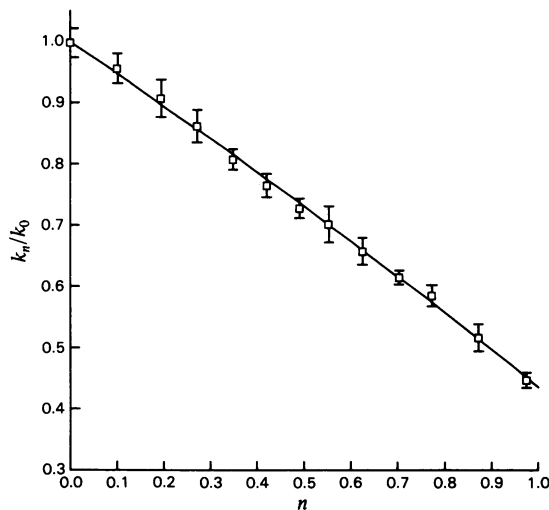


Fig. 1. Variation of k_n/k_0 with n for the papain-catalysed hydrolysis of Z-Lys-Nph at 25°C, pH 6.0

Each point represents four to six determinations (20 determinations at $n=0$) and error flags represent standard deviations. The solid curve is the best-fit curve determined by linear regression analysis for Model I, eqn. (4).

Table 1. Best-fit parameters for Model I, eqn. (4) for the papain-catalysed hydrolysis of Z-Gly-Nph, Z-Lys-Nph and Meo-Phe-Gly-Nph, determined by linear least-squares regression analysis

Error values are \pm s.e.m.

Substrate	k_0 (s ⁻¹)	ϕ_1^T	ϕ_2^T
Z-Gly-Nph*	5.21 \pm 0.04	1.009 \pm 0.049	0.443 \pm 0.024
Z-Lys-Nph†	38.68 \pm 0.22	1.086 \pm 0.039	0.401 \pm 0.017
Meo-Phe-Gly-Nph‡	7.63 \pm 0.05	1.054 \pm 0.046	0.420 \pm 0.020

* pH 7.0, 25°C, $[S]_0 = 9.32 \times 10^{-5}$ M, $[E]_0 = 3.23 \times 10^{-7}$ M, 4.55% (v/v) acetonitrile.

† pH 6.0, 25°C, $[S]_0 = 9.77 \times 10^{-5}$ M, $[E]_0 = 3.83 \times 10^{-8}$ M, 1.92% (v/v) acetonitrile.

‡ pH 7.0, 25°C, $[S]_0 = 6.23 \times 10^{-5}$ M, $[E]_0 = 2.66 \times 10^{-7}$ M, 2.38% (v/v) acetonitrile.

Thus it may be concluded that the dependence of the deacylation rate constant, k_n , upon n is best described by an essentially linear relationship, i.e. eqn. (3) with $\nu = 1$, $\phi_G = 1$, and $\phi^T = 0.40-0.44$, i.e. papain functions as a one-proton catalyst in deacylation. The implication of these results in terms of the mechanism of deacylation of papain-catalysed

hydrolyses may be analysed in detail as described in the Discussion section.

It is essential that the exchange with the solvent of all protons that participate in the reaction occurs rapidly. Brubacher & Bender (1966) have shown that when an aliquot of *trans*-cinnamoyl-papain made up in $^2\text{H}_2\text{O}$ is added to an H_2O buffer, no departure from first-order kinetics is observed throughout the reaction, and the deacylation rate constant is identical with that obtained when the sample is made up in H_2O . It follows that the exchange of any labile protons participating in the reaction is complete within the mixing time (approx. 10s), or does not occur at all. Similarly, if there is a conformational change of the acyl-enzyme upon deuteration which affects the deacylation rate, then it must be rapidly reversible. Schowen (1977) has argued against any gross conformational changes of proteins in $^2\text{H}_2\text{O}$. Other criticisms of the proton inventory technique have been raised (Kresge, 1973). For a discussion of the validity or otherwise of these criticisms, and a defence of the use of the proton inventory technique, see Schowen (1978) and also Elrod *et al.* (1975).

Discussion

Nature of protonic catalysis at the active site of papain

As argued in the Results section, the dependence of the deacylation rate constant, k_{cat} , upon n is essentially linear, and it may therefore be concluded that the kinetic isotope effect originates from the transfer of one proton in the transition state. However, the identification of the species between which proton transfer takes place can be made unequivocally only in conjunction with other experimental data.

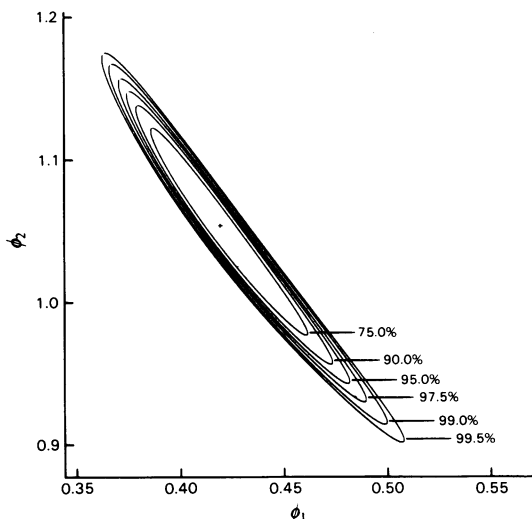


Fig. 2. Constant-confidence contours for Model I, eqn. (4), calculated from k_n values determined at various n values for the papain-catalysed hydrolysis of Meo-Phe-Gly-Nph at 25°C , pH 7.0

Each contour is the locus of ϕ_1 , ϕ_2 pairs satisfying eqn. (6), and is labelled with its level of significance. The cross represents the point defined by the best-fit values of ϕ_1 and ϕ_2 in Model I, eqn. (4).

Table 2. Best-fit parameters for model II, eqn. (7), for the papain-catalysed hydrolysis of Z-Gly-Nph, Z-Lys-Nph and Meo-Phe-Gly-Nph, determined by non-linear least-squares regression analysis

For experimental conditions see the footnotes to Table 1.

Substrate	k_0 (s^{-1})	ϕ_G	ϕ^T
Z-Gly-Nph	5.21 ± 0.04	0.991 ± 0.051	0.443 ± 0.025
Z-Lys-Nph	38.68 ± 0.22	0.910 ± 0.041	0.396 ± 0.020
Meo-Phe-Gly-Nph	7.64 ± 0.05	0.948 ± 0.048	0.419 ± 0.024

Table 3. Best-fit parameters for Model III, eqn. (8), for the papain-catalysed hydrolysis of Z-Gly-Nph, Z-Lys-Nph and Meo-Phe-Gly-Nph, determined by non-linear least-squares regression analysis

For experimental details see Table 1.

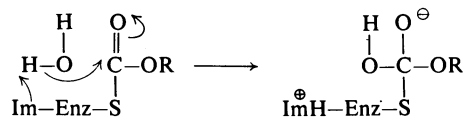
Substrate	k_0 (s^{-1})	ϕ	ω
Z-Gly-Nph	5.21 ± 0.04	0.435 ± 0.048	0.967 ± 0.123
Z-Lys-Nph	38.68 ± 0.22	0.354 ± 0.036	0.804 ± 0.072
Meo-Phe-Gly-Nph	7.64 ± 0.05	0.391 ± 0.044	0.872 ± 0.097

Thus it is apparent from the sigmoidal pH dependence of deacylation that the basic form of a group with pK_a approx. 4 is required for catalytic activity (Whitaker & Bender, 1965; Brubacher & Bender, 1966; Bender & Brubacher, 1966; Williams & Whitaker, 1967; Lowe, 1976; Zannis & Kirsch, 1978). This type of pH-dependence has been interpreted, in common with the serine proteinases, in terms of general base catalysis (Fersht, 1977). If the side chains of Cys-25 and His-159 exist in the free enzyme in the form of an ion-pair, and have pK_a values of approx. 4 and 8.6 respectively (Polgar, 1974; Lewis *et al.*, 1976; Johnson *et al.*, 1981a,b; Lewis *et al.*, 1981), the sulphur anion would be expected to be a good leaving group. This implies that tetrahedral intermediate breakdown will be fast and suggests that its formation will be rate-limiting.

The Hammett ρ value of 2.74 ± 0.32 found by Zannis & Kirsch (1978) for the deacylation of substituted benzoyl-papains is similar to that obtained for the deacylation of substituted benzoyl-chymotrypsins, suggesting a similar charge development in both reactions. They have contended on the basis of the magnitude of the ρ value that rate-limiting addition to the carbonyl group by an anionic nucleophile must occur in both enzymes (Asp-158 in papain and Asp-102 via the charge relay system in chymotrypsin) since reactions involving attack by uncharged nucleophiles are usually characterized by smaller (<1.4) ρ values. However, Johnson *et al.* (1981b) have shown that the size of the ρ value increases from this low value if the reaction is general-base-catalysed and also if the leaving group has a low pK_a . The larger Hammett ρ value is therefore consistent with general-base-catalysed attack.

From the above discussion it appears likely that in the deacylation of acyl-papains rate-limiting general-base-catalysed formation of the tetrahedral intermediate occurs. The most plausible candidate for the general base in the light of the X-ray structure (Drenth *et al.*, 1976) is the imidazole side chain of His-159. This conclusion is supported by recent ^1H n.m.r. studies in which His-159 was directly titrated in papain whose thiol group was blocked by an $-\text{S}-\text{CH}_3$ group (Johnson *et al.*, 1981a). The pK_a of His-159 in this model acyl-enzyme was found to be close to 4, in good agreement with that determined from pH-rate titrations. Zannis & Kirsch (1978) have argued in favour of Asp-158 as the general base, basing their argument on the Hammett ρ value of 2.74 and the near-zero heat of ionization observed for the deacylation of benzoyl-papains. However, using fluorometric titrations, Johnson *et al.* (1981b) have shown that the above observations are nevertheless consistent with His-159 acting as the general base (see also discussion above). If indeed His-159 is

the general base, then the rate determining step of deacylation may be written as follows:



HAR/PT diagram for the deacylation of acyl-papains

The mechanism as shown above is incomplete in that it does not define the structure of the transition state in terms of bond orders and atomic charges. In order to achieve this, it is necessary to specify the degree of proton transfer (PT) from water to imidazole, and the degree of heavy atom reorganization (HAR) (i.e. the extent of bond breaking and making to heavy atoms). The transition state structure may then be described by a point on a two-dimensional diagram relating HAR to PT. A third axis, orthogonal to the HAR and PT axes, represents the potential energy of the system. The general form of the potential energy surface may then be assessed from both the theoretical and experimental viewpoints in order to achieve sensible placing of putative reaction pathways (routes across the potential energy surface from reactants to products), intermediates (local potential energy minima) and transition states (saddle points on the potential energy surface). This method of describing reactions has become increasingly popular, particularly in the case of simple chemical reactions, and many such diagrams have recently been published in the literature (e.g. More O'Ferrall, 1970; Jencks, 1972; Alberly *et al.*, 1972; Cordes & Bull, 1974; Bruice, 1976; Hegazi *et al.*, 1978). The HAR/PT diagram for tetrahedral intermediate formation in the deacylation of acyl-papains is shown in Fig. 3. In order to encompass reasonable reaction mechanisms several possible alternative reaction pathways (P1-P5) are shown. P1 and P2 are pathways in which HAR and PT occur in separate steps of the reaction (either HAR followed by PT, as in P1, or PT followed by HAR, as in P2). Such pathways are described as being stepwise (often known as dynamically uncoupled). P1 and P2 are expected to proceed through the dipolar intermediates, I1 and I2, respectively. Pathways P3-P5, in which HAR and PT progress more or less in unison, are described as being concerted (or dynamically coupled) (Hegazi *et al.*, 1978). In order to achieve definition of the most likely transition state structure, it is necessary to consider a number of possible representative transition states. These are shown in Fig. 3 as T1-T9c. We proceed to the selection of the most reasonable transition state on the basis of a variety of experimental results

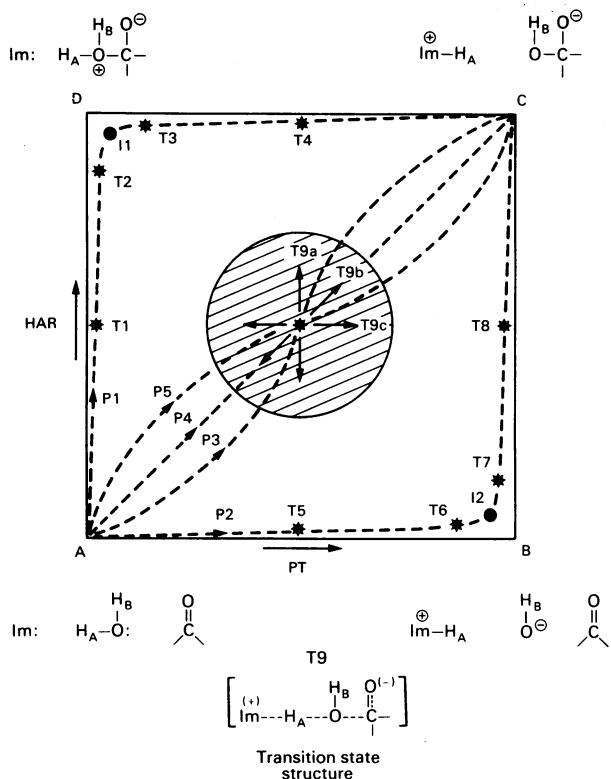


Fig. 3. Diagram which relates HAR to PT for the deacylation of papain

The species which are shown at the corners A and C represent the starting materials and products respectively. Any curve joining these two species describes a reaction pathway (dotted lines). Two step-wise pathways, P1 and P2, are shown passing close to the dipolar intermediates (●) I1 and I2 which are shown at D and B respectively. Three concerted pathways P3, P4 and P5, are shown which are on or near the diagonal joining A to C. Several alternative transition states (*) are shown on these pathways. Transition states T9a, T9b and T9c, which lie on pathways P3, P4 and P5 respectively, all have the same structure (which is shown at the bottom of the diagram) but differ in the degree of vibrational coupling between HAR and PT, and are expected to produce isotope effects of differing magnitude.

(including the proton inventory data reported here) and some theoretical considerations.

Location of transition state on HAR/PT diagram

Firstly, it is anticipated that the intermediates shown at the corners D and B, in Fig. 3, namely I1 and I2, will be unstable, since proton transfer to or from His-159 in these intermediates will be highly exergonic. [For this reason transition states T2, T3,

T6 and T7 have been included near these intermediates, in accordance with the Hammond Postulate (Hammond, 1955).] In view of the above, the minimum potential energy path, on which the transition state must lie, is then expected to be situated on or near the diagonal joining A and C, i.e. it will be concerted.

Albery (1975), on the basis of Jenck's rule for general acid-base catalysis (Jencks, 1972), has argued using Marcus theory (Marcus, 1968), that the transition state for proton transfer reactions occurs at a value of HAR such that the free energy change for proton transfer is zero. This condition is satisfied when the pK_a values of the proton-accepting and proton-donating species are equal, in which case $PT \approx 0.5$ for the transition state. If the pK_a of the intermediate I1 is similar to that of a protonated alcohol, say -2 , and pK_a is linearly coupled with HAR, then since the pK_a of water is approx. 15 and that of the imidazole side chain in the acyl-enzyme is approx. 4, proton transfer will be spontaneous when $HAR \approx (15 - 4)/(15 + 2) = 0.65$. Consequently the most plausible transition state will be located in the region of T9.

In accord with the above, Bronsted β values (and thus by implication degrees of PT) of 0.3–0.7 are generally found for carbonyl reactions exhibiting general acid-base catalysis (Wharton & Eisenthal, 1981). In particular, a value of 0.33 has been obtained (Fedor & Bruice, 1965) for the general base (including imidazole) catalysed hydrolysis of ethyl trifluoroethylacetate. This system represents a relevant model system for the deacylation of acyl-papains.

The large Hammett ρ value (2.74) obtained by Zannis & Kirsch (1978) for the deacylation of benzoyl-papains signifies a substantial accumulation of negative charge in the transition state, thus ruling out transition states T1–T3, in which the net negative charge is zero or very small, for which smaller Hammett ρ values are generally found (Johnson *et al.*, 1981b). Transition states T5–T7 may be likewise excluded since any effect of negative charge build-up on the incipient hydroxide ion will be poorly transmitted via the carbonyl group (to which it is not covalently bonded) to the benzoyl moiety (Exner, 1972).

In view of the above considerations a transition state in the region of T9 seems to be the most reasonable choice. We will now consider the extent to which the proton inventory results support this view.

In this regard, the magnitude of $\phi_{T_9} \sim 0.4$, which is responsible for the overall isotope effect of ~ 2.3 , merits discussion. Isotope effects considerably larger than this (5–8) are predicted by theory for a three-centre transition state model (in which the proton is located in a 'symmetric' position, i.e.

approximately half-transferred) (Westheimer, 1961; see also Schowen, 1972; More O'Ferrall, 1975). However, it has been pointed out by Bell (1965) and reiterated by several other authors (Johnson, 1967; Jencks, 1969; More O'Ferrall, 1975; Albery, 1975) that Westheimer's treatment using a three-centre model is inadequate for the description of proton transfer processes which involve concomitant heavy atom rearrangement, such as the reaction presently under discussion; at least a five-centre model must be considered. In such an extended structure it is necessary to consider additional transition state vibrations which involve motion of the proton in transit, some of which will be isotopically sensitive (i.e. their zero-point energy will decrease upon isotopic substitution). In a three-centre 'symmetric' transition state, in contrast, there are no isotopically sensitive vibrations. In the five-centre transition state, the zero-point energy decrease upon isotopic substitution of some of these extra vibrations will tend to cancel out that of the ground state vibration, resulting in a reduction in the expected isotope effect. Isotopically sensitive transition state vibrations can only exist, however, when the stretching vibrations of bonds to the hydrogen atom being transferred are strongly coupled to those of bonds to the migrating heavy atoms; the transition state is then described as being vibrationally coupled (often known as kinetically coupled). Transition states T9a, T9b, T9c all have the same structure (bond order, atomic charges etc.) (see bottom of Fig. 3) and are all situated on concerted reaction pathways (P3, P4 and P5 respectively), but they are characterized by different force fields (which are schematically represented by arrows), and thus differ in their degree of vibrational coupling. T9a represents a vibrationally uncoupled transition state in which the proton is in a stable potential well, and HAR dominates the reaction co-ordinate. The Schowens (1972, 1978) have maintained that this is in fact the mode of catalysis in general acid-base catalysed reactions. They have argued that the proton is not in the process of transfer in the transition state (being transferred partly before and partly after) and is therefore orthogonal to the reaction co-ordinate. Catalysis is effected by formation of a strong hydrogen bond to the reacting centre in the transition state, and is accordingly known as 'solvation catalysis'. They propose that such strong transition state hydrogen bonds may have fractionation factors of approx. 0.5. However, we argue [see also Albery (1975)] that the isotope effect expected for such a transition state would be significantly smaller than the observed isotope effect since the proton is not translating in the transition state. T9b represents a vibrationally coupled transition state in which compression of the Im-H bond facilitates extension of the H-O bond, which in turn facilitates compression of the O-C

bond; thus HAR and PT both contribute to the reaction co-ordinate. A larger isotope effect, but smaller than the maximum value predicted by the three-centre model, is expected in this case for the reasons outlined above. T9c represents a vibrationally uncoupled transition state, in which PT is the major component of the reaction co-ordinate. The maximum isotope effect predicted by theory for a 'simple' proton transfer in a three-centre transition state is expected in this case. Thus the isotope effect is predicted to increase to the maximum value in the order T9a, T9b, T9c. Albery (1975) has suggested

Table 4. Calculated proton inventories for transition states T1-T9c in Fig. 3.

The fractionation factors in this table for protons A and B (see Fig. 3), ϕ_A and ϕ_B , in T1-T9c were calculated using the HAR and PT co-ordinates shown below as follows. When proton A is translating in a 'symmetric' transition state (i.e. proton transfer is approximately half complete), as in T4, T5 and T9a-T9c, limits to ϕ_A were estimated as in Albery (1975) (see the Discussion). When proton A is translating in an 'asymmetric' transition state (i.e. proton transfer is either not very far advanced or is almost complete), as in T3 and T6, limits to ϕ_A were estimated as in Schowen (1972) (assuming that PT dominates the reaction co-ordinate). Secondary isotope effects for non-translating proton B were estimated by the following method, based on the treatment given in Schowen (1972). If HAR > PT (pathway P1), then $\phi_B = \phi(>OL^+)^{\Delta n} \cdot \phi(-OL)^{1-\Delta n}$ where $\Delta n = HAR - PT$ and $\phi(>OL^+) =$ fractionation factor of 'hydronium ion-like' proton = 0.69, $\phi(-OL) =$ fractionation factor of 'alcohol-like' proton = 1.0 (Albery, 1975). The fractionation factor of protonated imidazole is taken to be unity (Schowen, 1972). When proton A is not in the process of transfer (in T1 and T2) $\phi_A = \phi_B$. If PT > HAR (pathway P2), then $\phi_B = \phi(LO^-)^{\Delta n} \cdot \phi(-OL)^{1-\Delta n}$ where $\Delta n = PT - HAR$ and $\phi(LO^-) =$ fractionation factor of the hydroxide ion, ~ 0.5 (Schowen, 1972). If HAR = PT, as in T9a-T9c, $\phi_B \approx 1.0$ since bond order is conserved resulting in an 'alcohol-like' fractionation factor for proton B. (See structure of T9 at bottom of Fig. 3.)

Transition state	Approximate transition state fractionation factors		HAR/PT co-ordinates	
	ϕ_A	ϕ_B	PT	HAR
T1	0.8	0.8	0.0	0.5
T2	0.7	0.7	0.0	0.9
T3	0.4-0.9	0.7	0.1	1.0
T4	<0.3	0.8	0.5	1.0
T5	<0.3	0.7	0.5	0.0
T6	0.4-0.9	0.5	0.9	0.0
T7	1.0	0.5	1.0	0.1
T8	1.0	0.7	1.0	0.5
T9a	<0.3	1.0	0.5	0.5
T9b	0.3-0.7	1.0	0.5	0.5
T9c	>0.7	1.0	0.5	0.5

limits to the magnitude of the isotope effect expected in each case. These limits may be used to discriminate amongst the various alternatives. Thus $\phi_T < 0.3$ implies that a 'simple' proton transfer between two atoms is occurring, $0.4 < \phi_T < 0.7$ is indicative of vibrational coupling between HAR and PT, and $\phi_T > 0.7$ implies that the proton is not translating in the transition state. This allows the calculation of the expected proton inventories for transition states T1–T9c shown in Fig. 3. Secondary isotope effects, which must be included in the calculation, have been calculated by the method of Schowen (1972). Such secondary isotope effects arise from the contribution of grounded protons that experience a change in microenvironment during the reaction (see the 'Theory' section). Comparison of the hypothetical proton inventories, shown in Table 4, with the experimental results (Tables 1–3, Figs. 1 and 2) allows the rejection of all transition states other than T6, T7 and T9b. In T6 and T7, the non-translating proton (B) will have a hydroxide-ion like fractionation factor, i.e. $\sim 0.5^*$ and if the other proton (A) has a fractionation factor of, say, ~ 0.9 (e.g. if it is a translating proton in a very asymmetric transition state, nearly completely transferred as in T6) or ~ 1.0 (not translating, as in T7), then the predicted isotope results are consistent with experiment (see Fig. 2). However, T6 and T7 may be ruled out on the basis of theoretical considerations and structure–reactivity correlations (Bronsted and Hammett), see above.

Consequently, by a process of elimination, it may be postulated that the most reasonable transition state for the deacylation of acyl-papains is vibrationally well coupled and lies upon a concerted reaction pathway. This transition state is located in the region of T9b on the HAR/PT diagram, i.e. at

* Albery (1975) has contended that the fractionation factor of the hydroxide ion is approx. 1.2. If this is the case, then T7 is also excluded on the basis of the proton inventory data.

$HAR \approx PT \approx 0.5$. The shaded region in Fig. 3 represents the range of reasonable transition state structures. Table 5 summarizes the various results that have been combined to allow the characterization of the transition state.

The magnitudes of the Hammett ρ value, isotope effects etc. are very similar for deacylation reactions catalysed by serine proteinases. It follows that the above discussion applies equally well in this case and that the table for the serine proteinases corresponding to Table 5 for papain will be identical to the latter, and that the HAR/PT diagram for the serine proteinases will be similar to Fig. 3.

It remains to be seen whether more extended substrates (e.g. tripeptide derivatives) which would be capable of interacting more extensively with the protracted active site of papain (Lowe, 1976) than those used in this study might be able to induce dual proton transfer in a potential charge relay system, such as Asp(158)-His(159)-Cys(25). It must be mentioned, however, that there is now an increasing amount of evidence from a variety of n.m.r. studies (Markley, 1979) which is in contradiction to the charge-relay theory for the serine proteinases, and the recent 1H n.m.r. studies on papain (Johnson *et al.*, 1981a,b; Lewis *et al.*, 1981) support this view in the case of papain.

It is apparent from the results and discussion presented in this paper that the use of the proton inventory technique, particularly when combined with the results of other types of investigation, provides a powerful method for the determination of reaction pathways and transition-state structures in enzyme-catalysed reactions. The proton inventory method has been applied to the analysis of the acylation reaction in papain-catalysed hydrolysis; both the nature of the isotope effects and the resulting HAR/PT diagram are very different from those found for deacylation (R. J. Szawelski & C. W. Wharton, unpublished work).

The authors thank Dr. A. Cornish-Bowden for helpful discussions regarding the statistical analysis of the data.

Table 5. Summary of experimental and theoretical basis for the characterization of the most probable transition state in Fig. 3

Transition state	Hammett ρ value	Bronsted β value	Proton inventory	Theoretical prediction
T1	—	—	—	—
T2	—	—	—	—
T3	—	—	—	—
T4	+	+	—	—
T5	—	+	—	—
T6	—	—	+	—
T7	—	—	+	—
T8	+	—	—	—
T9a	+	+	—	+
T9b	+	+	+	+
T9c	+	+	—	+

References

- Albery, W. J. (1975) in *Proton Transfer Reactions* (Caldin, E. & Gold, V., eds.), chapter 9, Chapman and Hall, London
- Albery, W. J., Campbell-Crawford, A. N. & Curran, J. S. (1972) *J. Chem. Soc., Perkin Trans. 2*, 2206–2214
- Allen, K. G. D., Stewart, J. A., Johnson, P. E. & Wettlaufer, D. G. (1978) *Eur. J. Biochem.* **87**, 575–582
- Angelides, K. J. & Fink, A. L. (1978) *Biochemistry* **17**, 2659–2668
- Atkins, G. L. & Nimmo, I. A. (1973) *Biochem. J.* **135**, 779–784
- Bell, R. P. (1965) *Disc. Faraday Soc.* **39**, 16–24
- Bender, M. L. & Brubacher, L. J. (1966) *J. Am. Chem. Soc.* **88**, 5880–5889
- Blow, D. M., Birkoft, J. J. & Hartley, B. S. (1969) *Nature (London)* **221**, 337–340
- Box, G. E. P. & Hunter, W. G. (1962) *Technometrics* **4**, 301–318
- Brocklehurst, K. & Malthouse, J. P. G. (1978) *Biochem. J.* **175**, 761–764
- Brocklehurst, K., Malthouse, J. P. G. & Shipton, M. (1979a) *Biochem. J.* **183**, 223–231
- Brocklehurst, K., Herbert, J. A. L., Norris, R. & Suschitzky, H. (1979b) *Biochem. J.* **183**, 369–373
- Brubacher, L. J. & Bender, M. L. (1966) *J. Am. Chem. Soc.* **88**, 5871–5880
- Bruice, T. C. (1976) *Ann. Rev. Biochem.* **45**, 331–373
- Cordes, E. H. & Bull, H. G. (1974) *Chem. Rev.* **74**, 581–603
- Cornish-Bowden, A. (1976) *Principles of Enzyme Kinetics*, chapter 10, Butterworths, London
- Deslongchamps, P., Chenervert, R., Taillefer, R. J., Moreau, C. & Saunders, J. K. (1975) *Can. J. Chem.* **53**, 1601–1615
- Draper, N. R. & Smith, H. (1966) *Applied Regression Analysis*, John Wiley and Sons, New York, London and Sydney
- Drenth, J., Kalk, K. H. & Swen, H. M. (1976) *Biochemistry* **15**, 3731–3738
- Elrod, J. P., Gandour, R. D., Hogg, J. L., Kise, G. M., Maggiora, G. M., Schowen, R. L. & Venkatasubban, K. S. (1975) *Faraday Symp. Chem. Soc.* **10**, 145–153
- Elrod, J. P., Hogg, J. L., Quinn, D. M., Venkatasubban, K. S. & Schowen, R. L. (1980) *J. Am. Chem. Soc.* **102**, 3917–3922
- Exner, Q. (1972) in *Adv. Linear Free Energy Relat.* 1–69
- Eyring, H. (1935) *Chem. Rev.* **17**, 65–77
- Fedor, L. R. & Bruice, T. C. (1965) *J. Am. Chem. Soc.* **87**, 4138–4147
- Fersht, A. (1977) *Enzyme Structure and Mechanism*, chapter 5, W. H. Freeman, Reading
- Glascoc, P. K. & Long, F. A. (1960) *J. Phys. Chem.* **64**, 188–191
- Gold, V. (1972) *Adv. Phys. Org. Chem.* **7**, 259–331
- Hammond, G. S. (1955) *J. Am. Chem. Soc.* **77**, 334–338
- Hegazi, M. F., Quinn, D. M. & Schowen, R. L. (1978) in *Transition States of Biochemical Processes* (Gandour, R. D. & Schowen, R. L., eds.), chapter 10, Plenum Press, New York and London
- Hinkle, P. M. & Kirsch, J. F. (1970) *Biochemistry* **9**, 4633–4644
- Hopper, C. R., Schowen, R. L., Venkatasubban, K. S. & Jayaraman, H. (1973) *J. Am. Chem. Soc.* **95**, 3280–3283
- Hunkapiller, M. W., Forgac, M. D. & Richards, J. H. (1976) *Biochemistry* **15**, 5581–5588
- Jencks, W. P. (1969) *Catalysis in Chemistry and Enzymology*, McGraw-Hill, London
- Jencks, W. P. (1972) *Chem. Rev.* **72**, 705–718
- Johnson, F. A., Lewis, S. D. & Schafer, J. A. (1981a) *Biochemistry* **20**, 44–48
- Johnson, F. A., Lewis, S. D. & Schafer, J. A. (1981b) *Biochemistry* **20**, 52–58
- Johnson, S. L. (1967) *Adv. Phys. Org. Chem.* **5**, 237–330
- Kirsch, J. F. & Ingelstrom, M. (1966) *Biochemistry* **5**, 783–791
- Kresge, A. J. (1964) *Pure Appl. Chem.* **8**, 243–258
- Kresge, A. J. (1973) *J. Am. Chem. Soc.* **95**, 3065–3067
- Lewis, S. D., Johnson, F. A. & Schafer, J. A. (1976) *Biochemistry* **15**, 5009–5017
- Lewis, S. D., Johnson, F. A. & Schafer, J. A. (1981) *Biochemistry* **20**, 48–51
- Lowe, G. (1976) *Tetrahedron* **32**, 291–302
- Lowe, G. & Yuthavong, Y. (1971) *Biochem. J.* **124**, 107–115
- Marcus, R. A. (1968) *J. Phys. Chem.* **72**, 891–899
- Markley, J. L. (1979) in *Biological Applications of Magnetic Resonance* (Shulman, R. G., ed.), chapter 9, Academic Press, London
- More O'Ferrall, R. A. (1970) *J. Chem. Soc. B*, 274–277
- More O'Ferrall, R. A. (1975) in *Proton Transfer Reactions* (Caldin, E. & Gold, V., eds.), chapter 8, Chapman and Hall, London
- O'Leary, M. H., Yamada, H. & Yapp, C. J. (1981) *Biochemistry* **20**, 1476–1481
- Polgar, L. (1974) *FEBS Lett.* **47**, 15–18
- Quinn, D. M., Venkatasubban, K. S., Kise, M. & Schowen, R. L. (1980) *J. Am. Chem. Soc.* **102**, 5365–5369
- Schowen, R. L. (1972) *Prog. Phys. Org. Chem.* **9**, 275–332
- Schowen, R. L. (1977) in *Isotope Effects on Enzyme Catalysed Reactions* (Cleland, W. W., O'Leary, M. H. & Northrop, D. B., eds.), University Park Press, Baltimore
- Schowen, K. B. J. (1978) in *Transition States of Biochemical Processes* (Gandour, R. D. & Schowen, R. L., eds.), chapter 6, Plenum Press, New York
- Venkatasubban, K. S. & Silverman, D. N. (1980) *Biochemistry* **19**, 4984–4989
- Westheimer, F. H. (1961) *Chem. Rev.* **61**, 265–273
- Wharton, C. W., Cornish-Bowden, A., Brocklehurst, K. B. & Crook, M. (1974) *Biochem. J.* **141**, 365–381
- Wharton, C. W. & Eisenthal, R. (1981) *Molecular Enzymology*, chapter 2, Blackie and Son, Glasgow
- Whitaker, J. R. & Bender, M. L. (1965) *J. Am. Chem. Soc.* **87**, 2728–2737
- Williams, D. C. & Whitaker, J. R. (1967) *Biochemistry* **6**, 3711–3717
- Zannis, V. I. & Kirsch, J. F. (1978) *Biochemistry* **17**, 2669–2674